PHILOSOPHICAL TRANSACTIONS OF THE ROYAL SOCIETY A MATHEMATICAL, PHYSICAL & ENGINEERING SCIENCES

Dense Plasma in Z-pinches and the Plasma Focus

M. G. Haines

Phil. Trans. R. Soc. Lond. A 1981 **300**, 649-663
doi: 10.1098/rsta.1981.0093

Phil. Trans. R. Soc. Lond. A **300**, 649–663 (1981) [649]
Printed in Great Britain

Dense plasma in Z-pinches and the plasma focus

By M. G. Haines
Blackett Laboratory, Imperial College, London SW7 2AZ, U.K.

Many of the earliest experiments in controlled thermonuclear fusion research were Z-pinches. However these pinches were found to be highly unstable to the $m = 0$, the $m = 1$ (kink), and the Rayleigh–Taylor instability. The addition of an axial magnetic field and the removal of end losses by proceeding to a toroidal geometry has led to the class of discharges known as tokamaks and the reversed field pinch. But, at fusion temperatures and with practical values of applied magnetic field this restricts the plasma density to 10^{20} to 10^{21} m^{-3}, thereby requiring a containment time of several seconds and a plasma radius of about 1 m. Meanwhile studies of the plasma focus, which after its three-dimensional compression closely resembles a Z-pinch, have shown that a plasma of density 10^{25} m^{-3} and temperature 1 keV can be achieved in a narrow filament of radius 1 mm. It has enhanced stability properties which might be attributable to the effects of finite ion Larmor radius. Its neutron yield in deuterium can be as high as 10^{12} per discharge, with a favourable empirical scaling law, but the thermonuclear origin of the neutrons is doubtful because of the evidence of centre-of-mass motion and the formation of electron and ion beams. The development of high voltage, high current pulse technology has permitted the reconsideration of the Z-pinch to attain dense fusion plasmas which might be stabilized by scaling the ion Larmor radius to be comparable with the pinch radius. Experiments at Imperial College show that the plasma remains stationary for about twenty Alfven radial transit times, limited only by the period of the current waveform. Theory indicates that a dense compact Z-pinch can satisfy Lawson conditions with a power input dependent on the enhanced stability time, or, if stable, with ohmic heating balancing axial heat losses. Preliminary results on a laser-initiated Z-pinch are also presented.

1. Introduction

Many of the earliest experiments in controlled thermonuclear fusion research were Z-pinches. However they were found to be highly unstable to the $m = 0$ (sausage) and the $m = 1$ (kink) m.h.d. instabilities, and to the $m = 0$ Rayleigh–Taylor instability, see for example Carruthers & Davenport (1957) and Curzon *et al.* (1960), respectively.

The addition of a stabilizing magnetic field and the removal of end losses by proceeding to a toroidal configuration has led to the class of discharges such as tokamaks and the reversed field pinch. But if the magnetic field is limited to a practical value that can be produced conveniently by superconducting coils (5–10 T) then at fusion temperature and a plasma pressure less than the magnetic pressure ($\beta < 1$) this restricts the plasma density to 10^{20}–10^{21} m^{-3}. This dictates a containment time of several seconds, and, from diffusion processes, both classical and anomalous, requires a plasma radius of about 1 m.

Meanwhile studies of the plasma focus, which after its three-dimensional compression closely resembles a Z-pinch, have shown that a plasma of density 10^{25} m^{-3} and an electron temperature of 1 keV can be achieved in a narrow filament a few millimetres in diameter and about a centimetre in length. It sometimes can have enhanced stability properties which might be attributable to the effect of finite ion Larmor radius. Of greater interest is the very high neutron yield, up to 10^{12} neutrons per discharge, which greatly exceeds that of any other

fusion device. The yield appears to have an optimized value which scales as the pinch current I to the fourth power. The origin of the neutrons is still a matter for research, as under different conditions there is evidence of intense electron and ion beams, instabilities, turbulence and filamentations. All of these phenomena seem to be closely correlated to the neutron production which may not be thermonuclear in origin at all. In this paper the physical processes are discussed that could be playing an important role here.

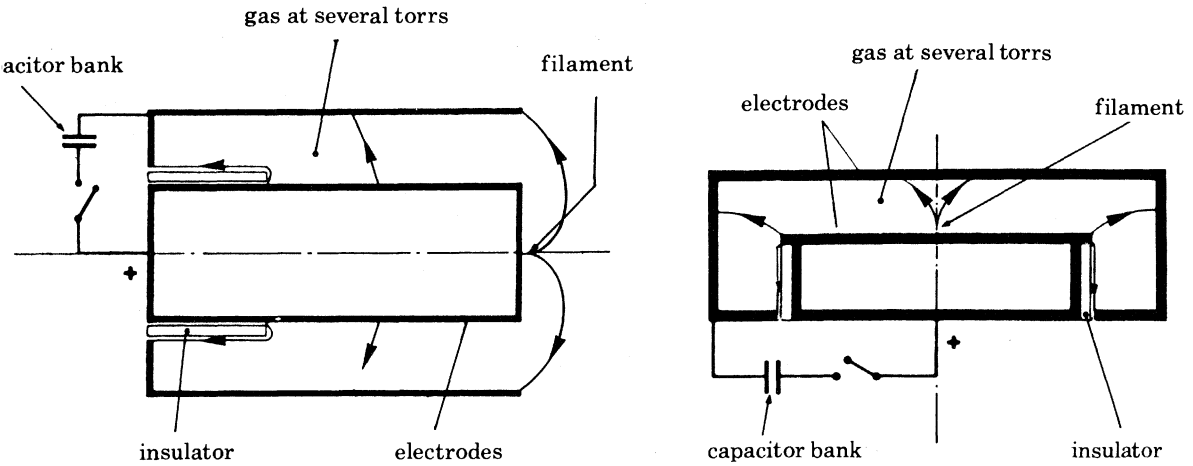

FIGURE 1. The two geometrical arrangements of the plasma focus: left due to Mather; right due to Filippov. (From Gentline *et al.* 1979.)

In the plasma focus the run-down phase allows the transfer of energy from the capacitor bank, at say 40 kV, to magnetic energy, which in turn permits an inductive voltage of ten or more times this to appear across the pinch at peak compression. However, in this device, the three-dimensional effects, including the axial flow and the complex phenomena associated with neutron production, could prevent a proper scaling to thermonuclear conditions. With the development of pulsed high voltage technology by Martin at A.W.R.E. (Aldermaston) it is now possible to return to the Z-pinch configuration with power sources corresponding to megavolts and megamperes for 100 ns or more. In this paper I review the experimental results at Imperial College and Los Alamos on the imploding Z-pinch and on a laser initiated gas-embedded Z-pinch. One important new idea here is the possibility of an extended period of stability through operating with ion Larmor radii comparable with the pinch radius. Indeed there is strong experimental evidence in support of this, and this is the régime most suited to satisfy Lawson conditions for the linear pinch.

2. PLASMA FOCUS

(*a*) *General features*

There are two commonly used geometrical arrangements of the plasma focus device, the 'Mather type' and the 'Filippov type' named after their inventors, and illustrated in figure 1. The first is long and has a central anode of small diameter, while the second is short with an anode of large diameter and a cathode that extends to the front of the anode. In both cases when the 20–50 kV capacitor bank is connected, break-down occurs along the insulator and the current sheet is driven by the $\boldsymbol{J} \wedge \boldsymbol{B}$-force away from the insulator towards the end of the

electrodes. The gas that is swept up by the moving front is ionized by the plasma and convected towards the outer cathode, so that, unlike a snowplough process in a linear pinch, there is no large accumulation of mass, but there is a build-up of magnetic (or inductive) energy. When the current sheet turns around the edge of the anode it is compressed to the axis with a velocity of 10^5 m/s to form a dense, hot current-carrying filament, several millimetres in diameter. Typical parameters are $n \approx 10^{25}\,\mathrm{m}^{-3}$, $T_e \approx 1$ keV.

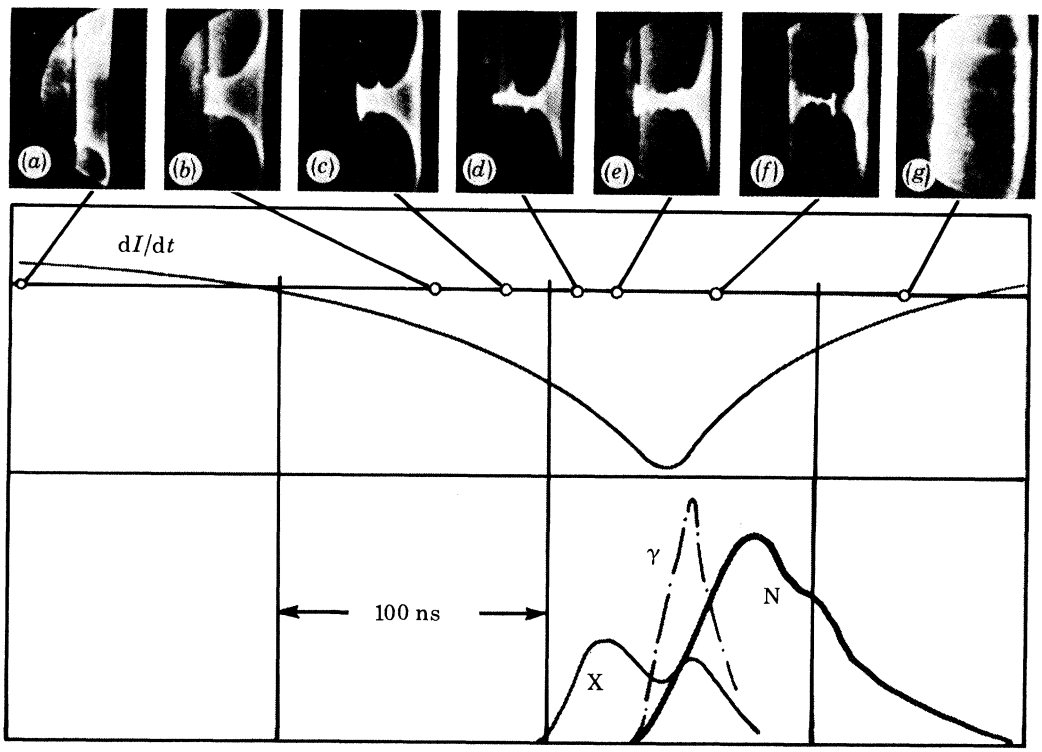

FIGURE 2. Sequence of side-on framing camera photographs illustrating the plasma structure against the rate of change of current $\mathrm{d}I(t)/\mathrm{d}t$, the soft X-ray pulse (X), the hard X-ray (γ) and the neutron emission (N). (From Decker & Wienecke 1976.)

A sequence of side-on optical framing pictures (exposure time 5 ns) is given in figure 2 (from Decker & Wienecke 1976). Frames (*a*) to (*d*) illustrate the first collapse to the axis which has an $m = 0$ Rayleigh–Taylor instability weakly present. Soft X-rays are emitted at this time, but very few neutrons. By frame (*e*) the pinch has expanded and then at (*f*) it has contracted again, going unstable simultaneously to a violent $m = 0$ instability in which the plasma column necks off in several places. At this moment, as indicated in figure 2 there is a burst of hard X-rays (50 keV–1 MeV energy) and the main neutron emission begins, with a f.w.h.m. pulse length of about 50 ns. Finally in frame (*g*) the plasma column has disrupted and the neutron emission ceases. The radial luminous hot plasma sheet is moving axially during this time preceded by an ionizing front which moves with a velocity of 10^6 m/s corresponding to ions of about 10 keV energy (Bernard 1976).

Plasma focus experiments operate over stored capacitive energy range of a few kilojoules to 1 MJ (Frascati). When each experiment is optimized with respect to filling pressure and electrode dimensions to give a maximum neutron yield, it is found that the yield Y varies as

the fourth power of the current in the pinched plasma, as shown in figure 3 over a wide range of experimental parameters. We will now examine other phenomena which could be associated with the neutron emission.

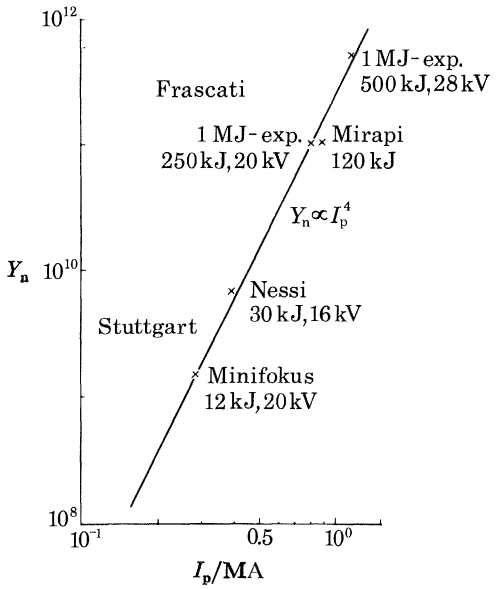

FIGURE 3. Optimized neutron yield against plasma current. (From Decker & Wienecke 1976.)

(*b*) *Electron and ion beams*

Most experiments now show the occurrence of energetic electron and ion beams at the time of the hard X-ray burst, the hard X-rays being caused by the bombardment of the anode by the electron beam or beams. Using the Ross filter method with absolutely calibrated detectors Bernard *et al.* (1978) showed that their 340 kJ facility at Limeil yields 150 J of X-radiation above 5 keV and peaking at 60 keV in 35 ns. From the data, the most consistent characteristics of the electron beam are an electron energy of 200–300 keV and current of 0.92–2 MA with a total energy content of 10–15 kJ and power of 0.4–0.8 TW. With regard to the ion beam,

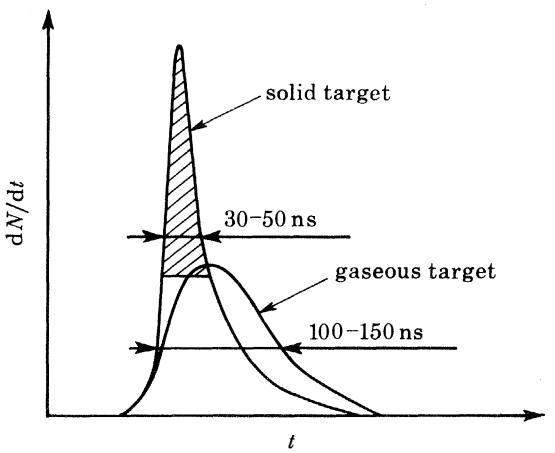

FIGURE 4. The rate of emission of neutrons with (shaded) and without a deuterated polyethylene target 25 mm from the anode. (From Bernard *et al.* 1978.)

Bernard *et al.* claim that it is the main source of neutrons, as the deuterons bombard both the dense gas and the ionized but relatively cold gas bubble between the ionization front and the shock front. The neutron spectra and flux are anisotropic and the emission zone has been identified as being in both the dense hot plasma and the lower density colder gas bubble. From these measurements it is consistent that the neutrons are produced by gas bombardment with an ion beam with deuterons of energy of about 300 keV, a current of 1.9 MA, energy 30 kJ and power 0.5 TW. When a deuterated polythene target is placed axially 25 mm from the anode the presence of the beam is confirmed quantitatively, as shown in figure 4, by the larger rate of neutron production lasting now only for 30–50 ns (the same time as for the electron beam and hard X-ray emission). The shortening of the pulse is because the deuterons in the beam lose all their energy in the solid in less than 1 ns while in the low density (*ca.* 2×10^{23} m^{-3}) gas they persist for the full transit time of tens of nanoseconds. The measured anisotropy, a ratio of three between simultaneous on-axis and 90° measurements, corresponds to a mono-energetic deuteron energy of 300 keV. The time of emission of the beams corresponds to a negative peak of $\mathrm{d}I/\mathrm{d}t$.

With the electron and ion beam energy and power being the same there is a large net momentum transferred in the direction of the ion beam. This can only be caused by a $J_r B_\theta$-force in a double sheath near the anode. We can consider a sheath of width less than the Larmor radius of a 300 keV deuteron across which is the voltage associated with $I\mathrm{d}L/\mathrm{d}t$ where L is the inductance of the plasma column. The magnetized electrons drift in the sheath with a $\boldsymbol{E} \wedge \boldsymbol{B}/B^2$ radial velocity, thus carrying the radial current J_r. Near the axis where B_θ goes to zero they will be ejected as a beam towards the anode. Using a hollow tubular anode, Nardi *et al.* (1978) detected this electron beam 10 cm behind the anode. The ions will be accelerated through the layer of high axial electric field. If the beam mechanism is dominant then the neutron yield should be strongly affected by a change of polarity. It is interesting to note that in the Limeil experiment the ion beam reaches the Alfvèn limiting current I_A for particles of energy eV, given non-relativistically by,

$$I_\mathrm{A} = \frac{4\pi}{\mu_0}\sqrt{\left(\frac{2mV}{e}\right)}. \tag{1}$$

Indeed much of the current thrust of research in the plasma focus is towards the optimization of the ion beam for bombardment of solid pellets in inertial confinement fusion. Under these conditions the ion beam is within an ion Larmor radius of the axis, and singular snake-like orbits are produced as calculated earlier by Potter & Haines (1971) to explain the anisotropic neutron production.

(*c*) *Turbulence*

Bernard *et al.* have reported density fluctuations 10^3 times thermal fluctuations in the rare plasma (*ca.* 10^{24} m^{-3}) surrounding the dense plasma. A ruby laser at right angles to the Z-axis was used to measure the scattering at 7°, 60°, 90° and 120° relative to the incident beam with spatial, angular and temporal (*ca.* 2 ns) resolution. With the scattering volume (10 mm × 0.8 mm) located 10 mm from the anode and 12.5 mm from the axis, it is found that the scattered spectrum $n_\mathrm{e} S_\mathrm{k}(\theta)$ is flat and thermal in all channels when the dense plasma crosses the volume. However, before the dense plasma sheet is in the scattering volume the rare plasma gives signals, but only at 7°, with a maximum in this cone at $\theta = 45°$ to the Z-axis. After the dense plasma has become a hot filament on the axis, the rare plasma off axis shows fluctuations

at about 10^3 times thermal fluctuations measured in the 7° channel with a maximum parallel to the X-axis. The author has measured a significant fraction of the total current in the rare plasma outside the dense region and attributes the turbulence to the current-driven two-stream, ion-acoustic instability or some other microscopic instability. It is difficult to see how the large $\boldsymbol{J} \wedge \boldsymbol{B}$ force in this rare plasma can be taken up by the plasma dynamics, and it is important that the magnetic probe measurements be confirmed by Faraday rotation of a probing laser (or by Zeeman splitting as done by Peacock & Norton (1975)).

In a later paper Bernard *et al.* (1979) state that the microscopic turbulence with its preferred wave direction is the cause of the high energies of the later beam formation. This is presumably thought to be a collective acceleration process. The anomalous impedence of the turbulent plasma column is in the range 0.2 to 0.4 Ω over a wide range of experiments. It is important to clarify how magnetic energy is converted to particle energy in the form of random or directed beams, and how the momentum is transferred to the ions if a beam is formed.

(*d*) *Isotropic neutron production*

In contrast to the work of Limeil, the Frascati group claim (Maisonnier & Rager 1979) that beam generation occurs only at low pressures and then only with a conversion efficiency of *ca.* 1%, yielding typically a 50 kA current. This lower pressure (*ca.* 1 Torr†) régime does not correspond to the régime for optimized neutron production which is at a pressure of 2–3 Torr, depending on the apparatus. The contribution of directed beams and anisotropic neutron spectra is only 20% according to these authors. Activation techniques using BN and graphite targets to interact with the deuteron were cross checked with LiH and LiD neutron emitting targets (fluxes being detected by silver activation and Geiger counters). The targets were placed at a rather large distance of 100–500 mm from the anode at various angles to the axis. Only ions with energy greater than 700 keV were detected by BN. These two factors make comparison with the Limeil results difficult. Perhaps at this great distance the ions would be deflected by the magnetic field in a high pressure discharge to give an apparently isotropic distribution, and at Limeil the dominant energy range of deuterons is 200–300 keV, outside the measurement here.

Until now two mechanisms have been postulated to account for neutron production: the beam-target mechanism and the moving quasi-thermonuclear boiler mechanism, the latter having energetic deuterons with an isotropic distribution. The Filippov geometry is considered to operate in the isotropic mode, but Bernard *et al.* (1978) found that there is no significant difference in the plasma dynamics or the neutron output between the two geometries. Those that advocate an isotropic ion distribution function claim that the turbulence in the low density (*ca.* 10^{24} m^{-3}) plasma is the origin of the stochastic heating to an ion temperature of *ca.* 50 keV.

(*e*) *Filaments*

Break-up of the current into several or many filaments has been frequently observed. Indeed the later beam formation can also occur at several localized regions, each with linear dimensions smaller than 10 mm (Nardi *et al.* 1979). Recently Gratton (1980) has reported the measurement of radial magnetic fields in the current sheath with random phase and of magnitude

† Torr = (101 325/760) Pa ≈ 133 Pa.

comparable with the driving B_θ-field, and has suggested that they are associated with filaments. The magnetic probes used were very small, about 0.3 mm in size, but measured a radial field component in the current sheet of one sign only. Gratton claims that only in discharges with radial magnetic field present are the high neutron yields found. He hypothesizes that the extra magnetic fields parallel and antiparallel to the main current give stabilized filaments at the time of the pinch, these fields being now B_z-components, and therefore that the neutrons are truly thermonuclear, originating from the small-scale, hot, stable filamentary structures. Fontan & Schifino (1980) have applied the theory of Tidman & Shanny (1974) on the thermomagnetic instability to explain the generation of these radial magnetic fields which occur if $\nabla n \cdot \nabla T_e > 0$ in the sheath. At low temperatures (high pressure) the stability will not theoretically occur and this is invoked to explain the absence of both radial magnetic field and neutrons at high filling pressures. A superficially similar break-up of a current sheet in the θ-pinch had been found by Dixon *et al.* (1973) but was explained by Haines (1974) in terms of an electrothermal instability with good agreement in wavelength variation with filling density.

If indeed stabilized filaments are necessarily present for neutron production it is a peculiar fact that when a stabilizing axial magnetic field is deliberately added to the plasma focus, its main effect is to reduce drastically the neutron yield and X-rays (Decker *et al.* 1978). Under the conditions of their small experiment (12 kJ) a magnetic field coil located in the inner electrode producing 5.5 mT causes an extinction of the main neutron pulse which was thought to be due to a beam-target mechanism.

Time-resolved soft X-ray pictures show that in the Filippov geometry there are hot-electron regions (Gentilini *et al.* 1979), and distinct focused electron streams detached from the outer boundary of the plasma column that produce hard X-rays (Gribkov *et al.* 1977).

(*f*) *Reconnection*

Recent unpublished results from Frascati (J. P. Rager 1980) show a new optical result: after the $m = 0$ instability the plasma tongues that move radially outwards reconnect convectively around the most pinched zone, forming bubbles of large dimensions. This could signify a tendency towards a relaxed, more stable state, the current density profile perhaps being flatter and allowing stability to the $m = 0$ interchange mode. This is seen to happen at a pressure of 5 Torr for a 250 kJ discharge when the optimum neutron yield is at 3 Torr, but at a higher energy of 400–500 kJ the reconnection occurs at 5–8 Torr when the neutron yield is optimized. There is evidence here then of a change of behaviour as a system optimized for neutron yield is taken to higher energy and pressure.

I conclude this section on the plasma focus by noting that there are many phenomena occurring, particularly associated with neutron production, beam production, turbulence, and filamentation, that need further study before a proper understanding of the experiments can be achieved.

3. Z-PINCH

(*a*) *General*

To obtain a velocity of compression that will yield fusion temperatures, or to ohmically heat a Z-pinch column to fusion temperatures, an applied voltage of the order of 10^6 V and a

current of 10^6 A is required. While early attempts were made by Heflinger & Leonard (1961) and by Adlam & Holmes (1963) based on a proposal of J. E. Allen & J. H. Adlam (private communication), it was not until the recent development of high voltage pulse technology and the speculation of large ion Larmor radius stabilization that a new approach to Z-pinches was possible.

In this paper I will report on two types of Z-pinch studied at Imperial College, one based on the fast compression of a pre-ionized gas, and the other a laser initiated gas embedded pinch which is also being studied at Los Alamos. These pinches have a high rate of power input and show remarkable properties of stability and high density.

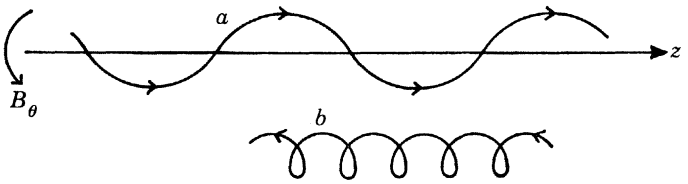

FIGURE 5. Sketch of a singular (on-axis) ion orbit and an off-axis guiding orbit. (From Haines 1978.)

(*b*) *Theory*

It is well known that finite ion Larmor radius (f.L.r.) effects can stabilize weakly unstable m.h.d. configurations. Potter (1971) in a numerical simulation showed that the addition of f.L.r. terms in the stress tensor can delay the onset of the $m = 0$ instability in a plasma focus, while the generalized cylindrical problem has been solved from the Vlasov equation for small a_i/a by Wright *et al.* (1976). The case of large Larmor radius, $a_i \approx a$, is currently being studied numerically at Imperial College. The axis where we have $B_\theta = 0$, however, provides a singularity. Indeed complex particle orbits can occur and it can be shown (Haines 1978) that for each species i there is a singular axial current flow I_{si} within one Larmor radius of the axis given by

$$I_{si} = \frac{4\pi}{\mu_0}\left(\frac{P_{\perp i}}{J_z}\right)_{r=0}, \tag{2}$$

where $P_{\perp i}$ is the perpendicular pressure and J_z the total current density, both evaluated at the axis. I_{si} is essentially the return diamagnetic current, and for equal electron and ion temperatures is typically about half the total current flow. A singular and an off-axis guiding-centre orbit are shown schematically in figure 5.

Therefore when considering end losses, the singular thermal flow down the axis is important. However whether the end losses are due to electron thermal conduction, electron convection by current flow or by singular and guiding centre ion flow we obtain much the same result for an equilibrium Z-pinch that satisfies the Lawson conditions (Haines 1978). Balancing ohmic heating against radiation and end losses, and choosing $n\tau = 5 \times 10^{20}$ m^{-3} s, $T_e = T_i = 3 \times 10^8$ K, where τ is the energy confinement time, we obtain typically a voltage of 6.5×10^4 V, a current I of 0.97 MA and a line density N of 5.6×10^{18} m^{-1}. This satisfies the Bennett relation for pressure balance:

$$\mu_0 I^2 = 8\pi N k(T_e + T_i), \tag{3}$$

and leads the ratio of the mean ion Larmor radius a_i to pinch radius a, from

$$a_i/a = 8.08 \times 10^8/N^{\frac{1}{2}}, \tag{4}$$

to be 0.34. This shows that a fusion Z-pinch is in a régime of large ion Larmor radius which could lead to much enhanced stability. The ratio of drift velocity to ion sound speed is similar to a_i/a, and ion sound turbulence is therefore unlikely to occur unless T_i is much less than T_e. One free parameter remains to be chosen, namely the length of the discharge z_0, the pinch radius a, the mean number density $\bar{n}$, or the confinement time τ. A range of consistent values is shown in table 1. We note that the pinch has to be dense and very narrow. If the α particles are to be contained, a larger current and a smaller ratio of a_i/a is required, which may not possess such favourable stability properties.

TABLE 1. RANGE OF CONSISTENT VALUES OF z_0, a, $\bar{n}$ AND τ

z_0/m	a/μm	$\bar{n}$/m^{-3}	τ/s
10	201	4.46×10^{25}	1.12×10^{-5}
1	63.4	4.46×10^{26}	1.12×10^{-6}
0.1	20.1	4.46×10^{27}	1.12×10^{-7}
0.01	6.34	4.46×10^{28}	1.12×10^{-8}

If the plasma column is not stable and the energy loss is determined by convection of plasma with a time $\tau_c = M\tau_s$, where M is a number in excess of unity and τ_s is the radial ion sound time or the fastest m.h.d. instability growth time, then the required power input IV is given by

$$IV = \frac{4\pi z_0 (kT)^2}{m_i} \frac{n\tau_c}{M}, \tag{5}$$

(Choi *et al.* 1979). In our compression experiments it is found that the plasma is stable for the duration of the discharge, showing that M is at least 20, owing probably to finite ion Larmor radius effects. An M-value of 10^3 or more is required.

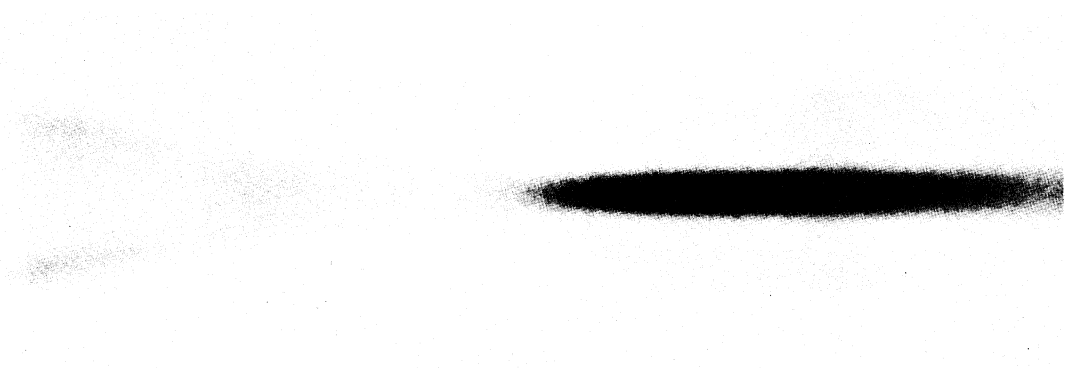

FIGURE 6. End-on streak picture in the Imperial College Mark II Z-pinch; pressure 70 mTorr H_2, current 60 kA, in Pyrex tube 8 cm long, 4 cm diameter.

(c) *Compression Z-pinch experiments*

We can illustrate the enhanced stability in figure 6 which is a streak picture taken end-on in our Mark II Z-pinch (800 kV, 120 kA, 120 ns transmission line configuration). We can identify an initial shock front with a velocity of 3×10^5 m s^{-1} that reaches the axis in 50 ns followed by the current-carrying piston. The final radius is about one-third of the tube radius, in keeping with a slug model by Potter (1978) and the electrical measurements. The absence of a bounce has been found in a one-dimensional Lagrangian computer model (Choi *et al.* 1979)

to be due to the viscous dissipation of the directed motion when the Reynolds's number is not small. Earlier results were reported in Choi *et al.*; we will concentrate on more recent work. Figure 7 shows the Mark II device set up for holographic interferometry by means of a 30 mJ, 5 ns ruby laser in an end-on double-pass configuration. Figure 8 shows a hologram taken 350 ns after the start of the current showing a well defined stable column still persisting after several cycles of the current.

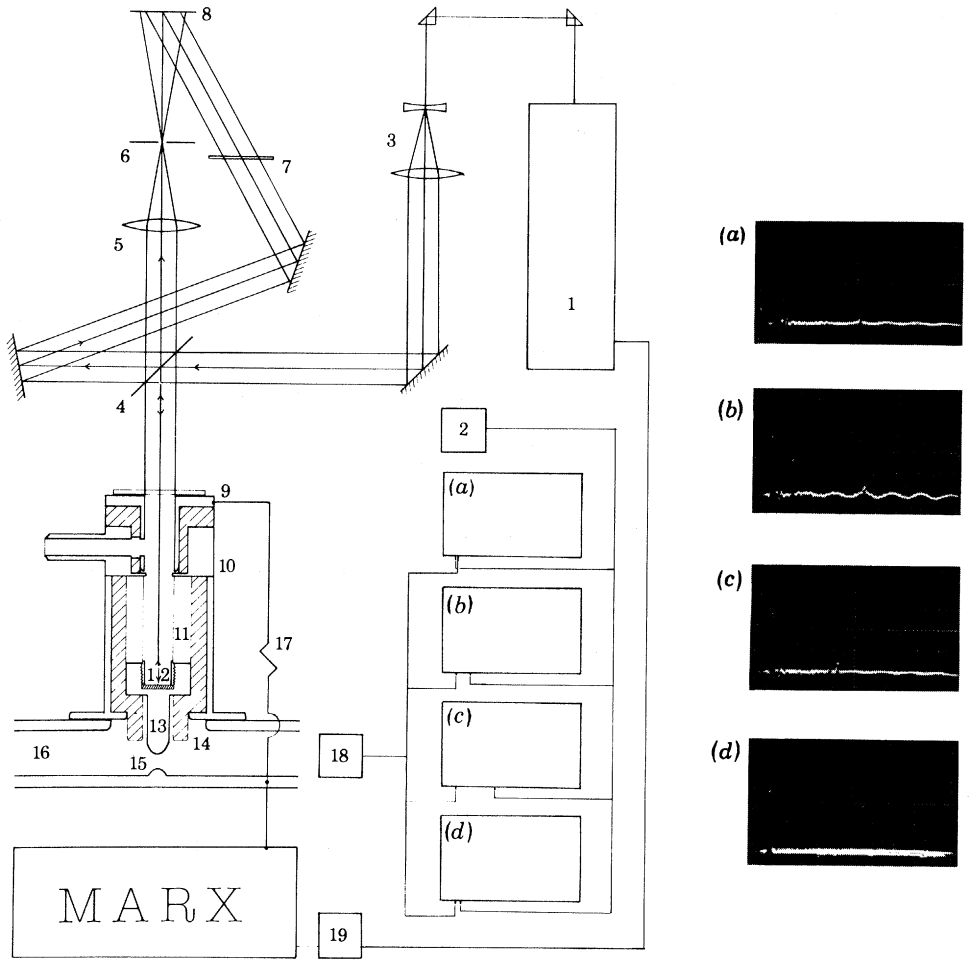

FIGURE 7. Arrangement for holographic interferometry. 1, Q-switched 30 mJ ruby laser; 2, pin diode laser monitor; 3, beam-expanding optics; 4, beam splitter; 5, imaging lens; 6, aperture; 7, beam alternator; 8, IOE75 film; 9, pre-ionization electrode; 10, Earth electrode; 11, pinch tube; 12, front surfaced mirror; 13, main electrode; 14, PTFE insulator; 15, water gap; 16, transmission line PFL; 17, $CuSO_4$ resistor; 18, water-gap optical monitor; 19, optical trigger to laser Pockel cell. Oscillographs (*a*)–(*d*) correspond with holograms (*a*)–(*d*) in figure 9.

A series of holograms in figure 9 were obtained on the 1 cm radius pinch tube. A filling density of 300 mTorr H_2 was used for the upper sequence (*a*) to (*c*) giving corresponding density profiles in (*f*), curve 1 being 73 ns (*a*), curve 2, 305 ns (*b*), and curve 3, 676 ns (*c*) after the start of the current. Figure 9(*d*) is a hologram taken on the 0.5 cm radius tube at a filling pressure of 1 Torr H_2 192 ns from the start of the pinch. Figure 9(*e*) shows the corresponding density profiles (1) 160 ns and (2) 218 ns after the start of the current. In figure 7 the timing oscillographs are displayed corresponding to the holograms (*a*)–(*d*) of figure 9.

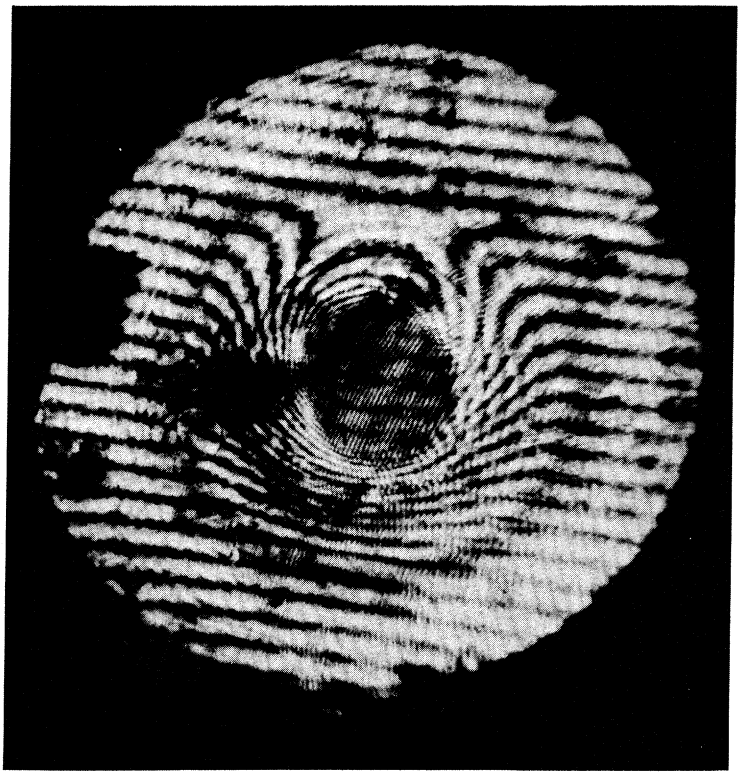

FIGURE 8. Holographic interferographic picture 350 ns after start of the current; tube radius 1 cm, length 5 cm, fill pressure 350 mTorr H_2, current 80 kA.

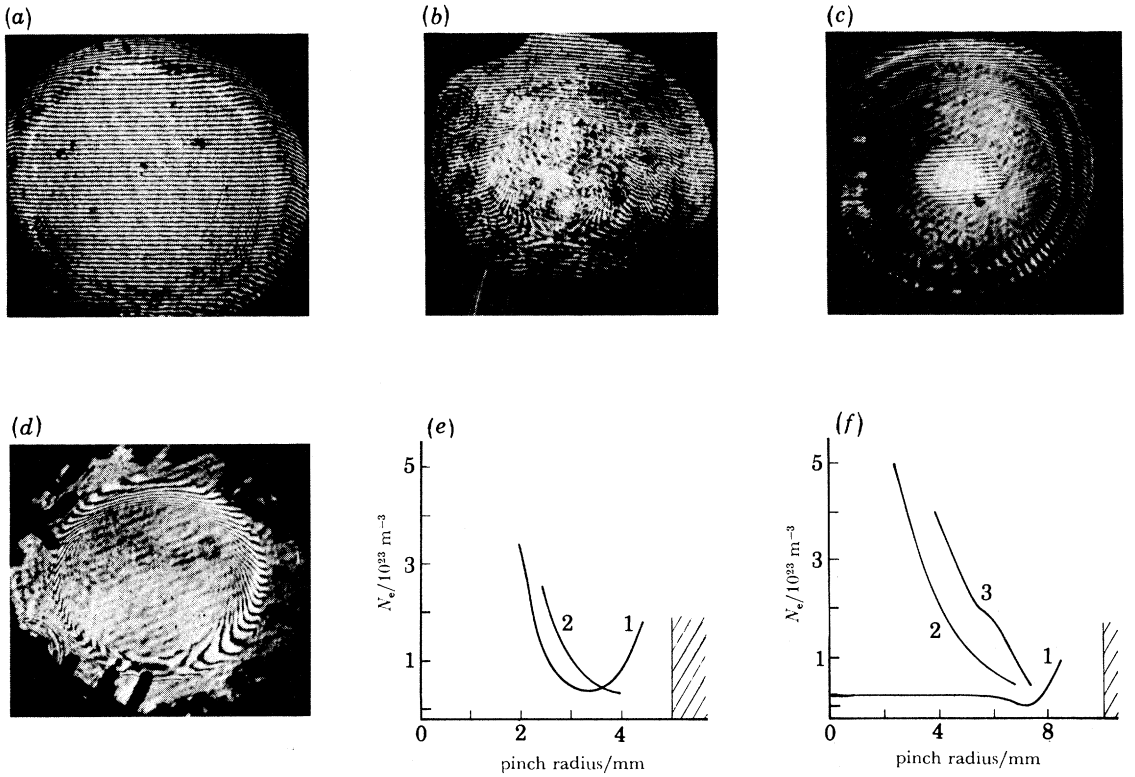

FIGURE 9. Series of holograms and density profiles (see text). The electron density profiles were calculated from the holograms by neglecting the contribution of neutrals to the refractive index.

PHILOSOPHICAL TRANSACTIONS OF THE ROYAL SOCIETY A MATHEMATICAL, PHYSICAL & ENGINEERING SCIENCES

Temperature estimates have been made with added nitrogen impurity, and by examining the broadening of the He^{II} 468.6 nm line in a helium discharge. The latter gave 100 eV, while in the former case the N^{4+} line appeared after 200 ns.

The smaller Mark I device (200 kV, 80 kA, 150 ns Blumlein configuration) had a quartz tube 10 cm long and 2 cm radius which allowed side-on framing photography, as illustrated in figure 10 in 200 mTorr H_2 plus 10% air at 50 ns per frame. (In pure H_2 at low filling pressure the emission is too low for the camera available.) The collapse is axially uniform and the pinch remains grossly stable. A new K_α emission technique using two small targets of different materials enabled the electron temperature to be measured. At 30 mTorr H_2 an electron temperature of 1.0 ± 0.2 keV was found.

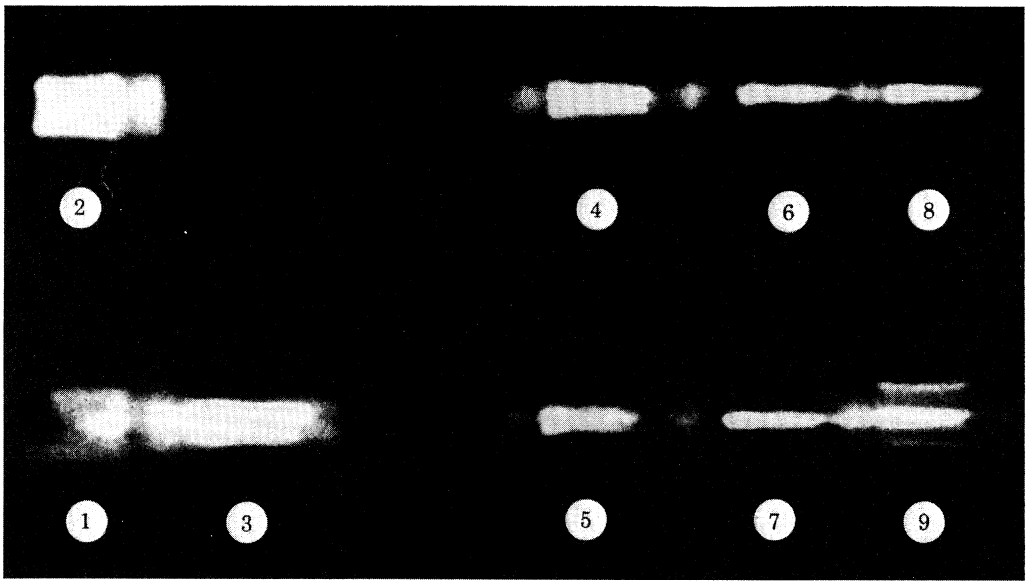

FIGURE 10. A sequence of side-on framing camera photographs taken on the Mark 1 *Z*-pinch. The exposure time is 10 ns, with 50 ns between successive exposures numbered in sequence. In each frame the light at each end of the main discharge is due to the pre-ionizers.

Future work requires the testing of the stability at higher currents and for longer times. Better measurements of temperature and impurity content are also needed.

In the longer term the further adiabatic compression to high density should be studied by using a programmed rising current. The current objectives have included the scaling of the collapse time with filling density, tube radius and current to test the correctness of the theory.

(*d*) *Gas-embedded laser initiated Z-pinch*

The extremely high densities and small pinch radii required, as shown in table 1, made it clear that as an alternative to compressing a plasma to these values it might be possible to initiate a pinch at these conditions, by using a focused laser to form a narrow ionizing channel, and to heat it up under pressure balance by the ohmic current. Haines (1960) studied this heating problem and found that the heating time is comparable with the final confinement time required for fusion. A high initial rate of rise of current is required, for which a low inductance line is most suitable.

A small pilot experiment has been operating at Imperial College in which a 1 J Nd–glass laser of pulse length 1 ns is focused with a large *f*-number lens through a hollow electrode on to the axis of a *Z*-pinch tube. The small Marx generator and line delivers 15 kA for 20 ns to a discharge tube 2 cm in length. This is switched on after the laser has weakly ionized a region of radius of about 100 μm. The discharge forms here, and figure 11 illustrates a sequence of

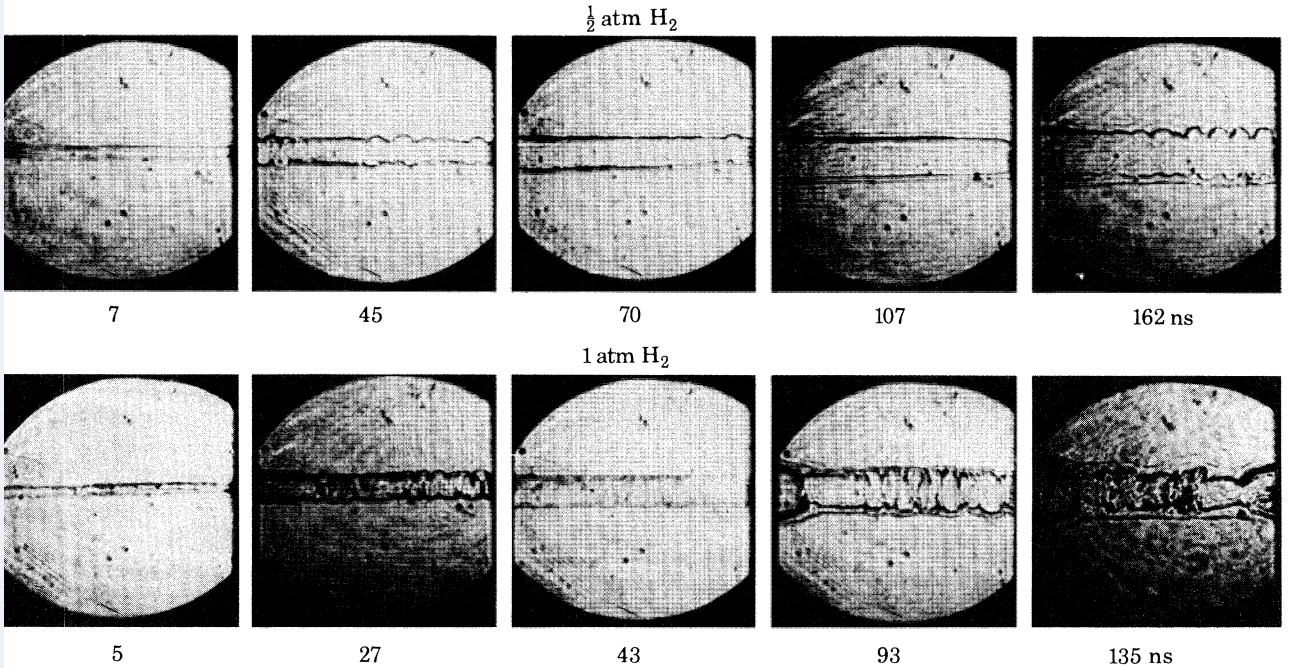

FIGURE 11. Sequence of side-on Schlieren interferograms, upper five at ½ atm H_2 and lower five at 1 atm H_2 (see text).

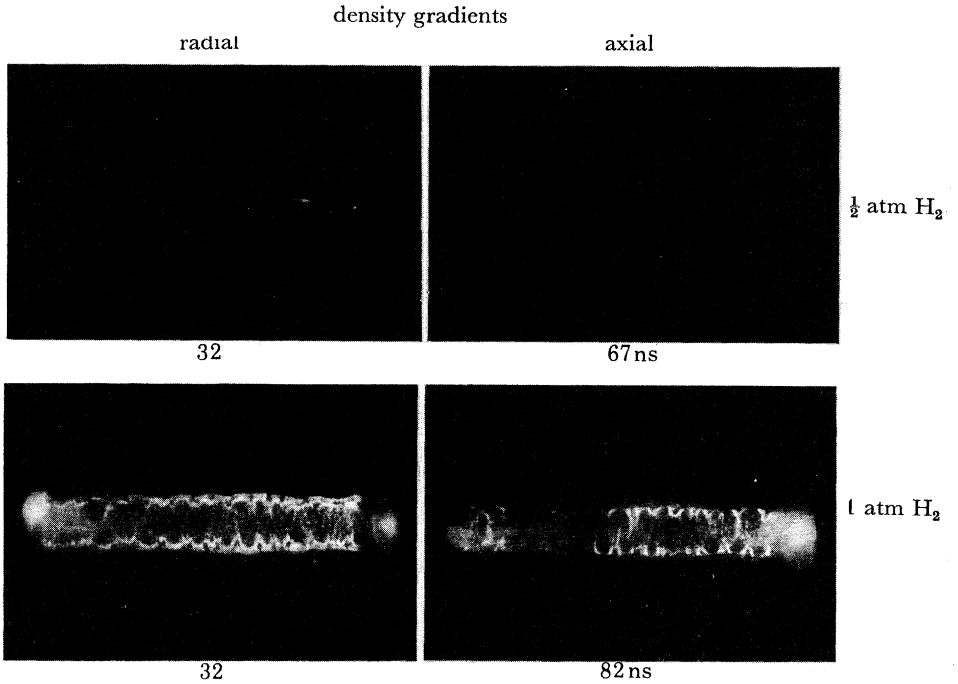

FIGURE 12. Dark-field schlieren interferograms of laser-initiated gas-embedded *Z*-pinch (see text).

five Schlieren interferograms with the use of Q-switched 5 ns ruby laser pulses, looking side-on the discharge, and taken at $\frac{1}{2}$ atm†. Another sequence is shown for 1 atm pressure H_2. At the lower pressure the column is essentially stable and expands slowly until at 162 ns it is about 3 mm in radius. At the higher pressure a helical instability is formed but the helix is tight and the plasma column remains well defined. With masking edges in either the radial or axial direction, we can examine the radial or axial density gradients independently. In the upper left dark field image of figure 12, taken at $\frac{1}{2}$ atm H_2 at 32 ns, a uniform pinch column is observed. No image appears on the upper right-hand side, showing that there is no axial density gradient. However the corresponding results for 1 atm show both radial and axial gradients in the tight helical deformation. This helical configuration could well be the minimum energy state (Lieberman 1979, private communication). The stability of the lower pressure case is probably due to finite Larmor radius effects which, from equation (4), are more important at low line density.

The laser-initiated Z-pinch in H_2 at Los Alamos (L. A. Jones 1980, private communication) also shows a growth of a helical structure in a radially expanding column. X-ray spectroscopy gave a temperature of 55 eV, 100 ns after a rapid rise to 40 eV. Experiments have also been conducted in up to 3 atm of He or N_2, the developing structures for which were rather different. This experiment is powered by a 600 kV, 70 kJ Marx generator and line with a 200 ns current pulse.

These experiments are preliminary, but very promising for the attainment of dense stable plasmas with no wall interaction. We could indeed envisage a reactor system in which liquid lithium acts as a moderator, first wall, breeder and return conductor. A high pressure D–T gas bubble is blown through a hollow electrode until it extends to the other electrode. The focused laser pulse is applied, followed by the high current source for a few hundred nanoseconds – a rather simple concept. Indeed there may be no need for a second electrode, the lithium on axis fulfilling this function.

4. Summary

We have seen that the plasma focus is rich in phenomena and that there are many proposed mechanisms for neutron production. A simplified interpretation could be that at a high line density it is violently m.h.d. unstable, but can form reconnecting bubbles. Because of the axial plasma flow the line density drops continuously, so passing through the finite Larmor radius enhanced stability region and into a region of lower line density where current induced turbulence is important. Filamentation could be important here, but at even lower line densities the discharge will behave as a magnetic diode breaking up into separate electron and ion beams.

The aim of the Z-pinch work is to operate as a dense, hot thermonuclear plasma by using large ion Larmor radius effects for stabilization or at least to make the energy loss through instabilities acceptable. Two routes are being explored: the compression of the column to high densities; and the ohmic heating of a laser-initiated high-pressure gas-embedded pinch. Both methods are yielding promising results on the gross stability of the discharges for tens of Alfven radial transit times.

The author is grateful to Dr A. Bernard (Limeil), Professor Dr G. Decker (Düsseldorf), Dr J. P. Rager (Frascati), Professor H. Herold (Stüttgart), Dr L. A. Jones (Los Alamos), Dr

† atm = 101 325 Pa.

PHILOSOPHICAL TRANSACTIONS OF THE ROYAL SOCIETY A MATHEMATICAL, PHYSICAL & ENGINEERING SCIENCES

N. Peacock (Culham) and Professor F. Gratton (Buenos Aires) for sending him their latest results, and to Dr D. E. Potter, Mr P. Choi, Mr A. E. Dangor and Dr A. Dymoke-Bradshaw for discussions and for making available new experimental results from Imperial College.

References (Haines)

Adlam, J. M. & Holmes, L. A. 1963 *Nucl. Fus.* **3**, 62–74.

Bernard, A. 1976 *Pulsed high beta plasmas* (ed. D. E. Evans), pp. 69–86. Oxford: Pergamon Press.

Bernard, A., Garçonnet, J. P., Jolas, A., Le Breton, J. P. & de Mascureau, J. 1979 *3rd International Conference on High Power Electron and Ion Beam Research and Technology*, Novosibirsk, U.S.S.R., 3–6 July 1979, vol. I, pp. 269–276. Novosibirsk: Institute of Nuclear Physics.

Bernard, A., Garçonnet, J. P., Jolas, A., Le Breton, J. P. & de Mascureau, J. 1979 *Plasma Physics and Controlled Nuclear Fusion Research* 1978, vol. 2, pp. 159–172. Vienna: I.A.E.A., also *International Conference on Energy Storage, Compression and Switching*, Venice, December 1978. (To be published.)

Carruthers, R. & Davenport, P. A. 1957 *Proc. phys. Soc.* **70**, 49–50.

Choi, P., Dangor, A. E., Folkierski, A., Kahan, E., Potter, D. E., Slade, P. D. & Webb, S. J. 1979 *Plasma Physics and Controlled Nuclear Fusion Research* 1978, vol. 2, pp. 69–79. Vienna: I.A.E.A.

Curzon, F. L., Folkierski, A., Latham, R. & Nation, J. A. 1960 *Proc. R. Soc. Lond.* A **257**, 386–400.

Decker, G. & Wienecke, R. 1976 *Physica* C**82**, 155–164.

Dixon, R. M., Duchs, D. F. & Elton, R. C. 1973 *Physics Fluids* **16**, 1742–1744.

Fontán, C. F. & Schifino, A. S. 1980 *International Conference on Energy Storage, Compression and Switching*, Venice, December 1978. (To be published.)

Gentilini, A., Maisonnier, Ch. & Rager, J. P. 1979 *Comments Plasma Phys.* **5**, 41–54.

Gratton, F. 1980 Magnetic structures and the neutron yield of the dense plasma forms. Invited paper at 'Emerging Nuclear Energy Systems', April 1980, Lausanne.

Gribkov, V. A., Dubrovskiĭ, A. V., Isakov, A. I., Kozlova, T. A., Krokhin, O. N., Nikulin, V. Ya., Semenov, O. G. & Sklizkov, G. V. 1977 *JETP Lett.* **26**, 209–214.

Haines, M. G. 1960 *Proc. phys. Soc.* **76**, 250–260.

Haines, M. G. 1976 *J. Plasma Phys.* **12**, 1–14.

Haines, M. G. 1978 *J. Phys.* D **11**, 1709–1720.

Heflinger, L. O. & Leonard, S. L. 1961 *Physics Fluids.* **4**, 406–423.

Maissonier, Ch. & Rager, J. P. 1979 *3rd International Conference on High Power Electron and Ion Beam Research and Technology*, Novosibirsk, U.S.S.R., 3–6 July 1979, vol. I, pp. 233–269. Novosibirsk: Institute of Nuclear Physics.

Nardi, V., Bostick, W. M., Feugeas, J., Prior, W. & Cortese, C. 1979 *Plasma Physics and Controlled Nuclear Fusion Research* 1978, vol. 2, pp. 143–157. Vienna: I.A.E.A.

Peacock, N. J. & Norton, B. A. 1975 *Phys. Rev.* A **11**, 2142–2146.

Potter, D. E. 1971 *Physics Fluids.* **14**, 1911–1924.

Potter, D. E. 1978 *Nucl. Fus.* **18**, 813–823.

Potter, D. E. & Haines, M. G. 1971 *Plasma Physics and Controlled Nuclear Fusion Research* 1971, vol. 1, pp. 611–620. Vienna: I.A.E.A.

Tidman, D. A. & Shanny, R. A. 1974 *Physics Fluids.* **17**, 1207–1210.

Wright, R. J., Pott, D. F. R. & Haines, M. G. 1976 *Plasma Phys.* **18**, 1–26.

PHILOSOPHICAL TRANSACTIONS OF THE ROYAL SOCIETY A MATHEMATICAL, PHYSICAL & ENGINEERING SCIENCES

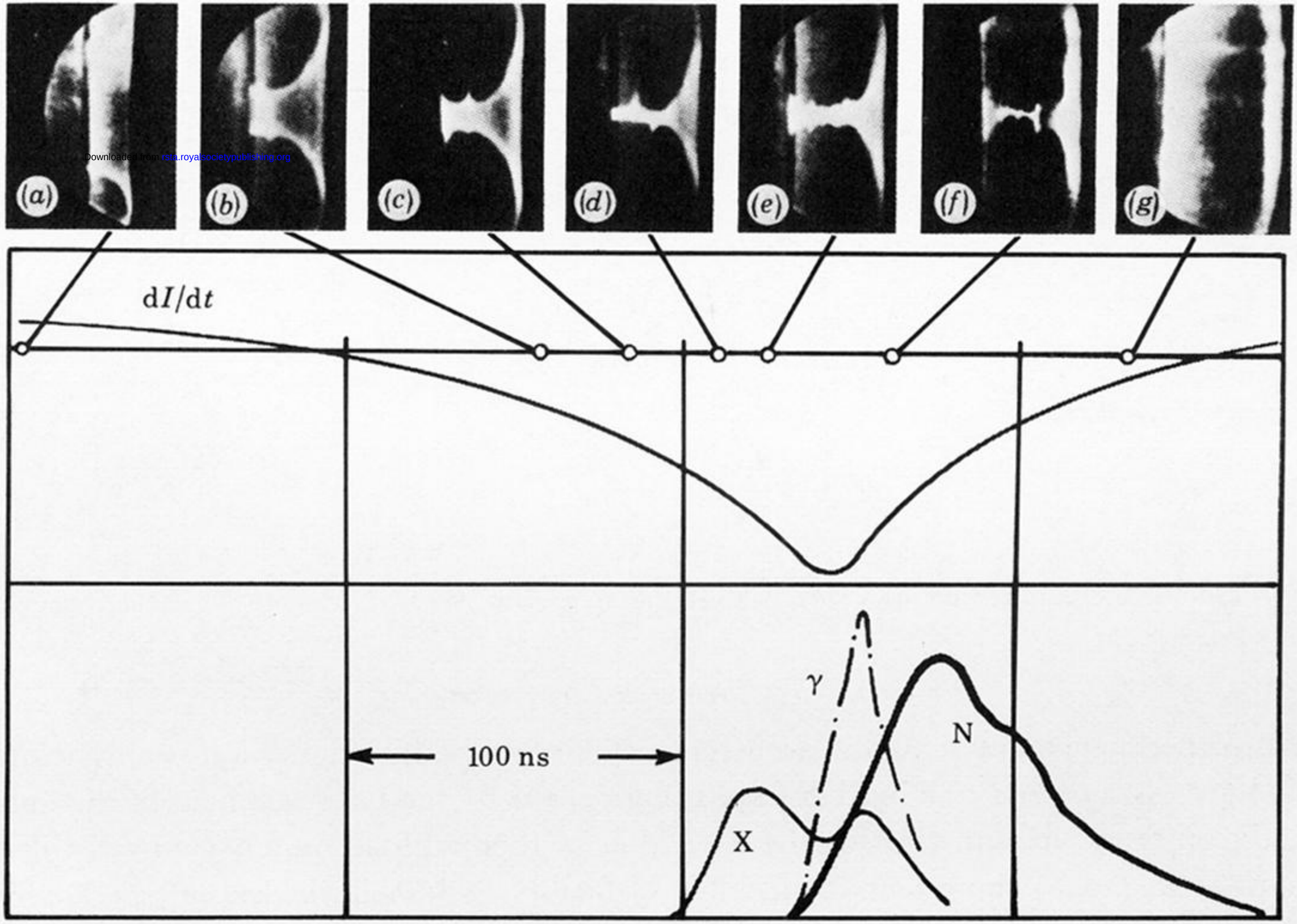

GURE 2. Sequence of side-on framing camera photographs illustrating the plasma structure against the rate of change of current $dI(t)/dt$, the soft X-ray pulse (X), the hard X-ray (γ) and the neutron emission (N). (From Decker & Wienecke 1976.)

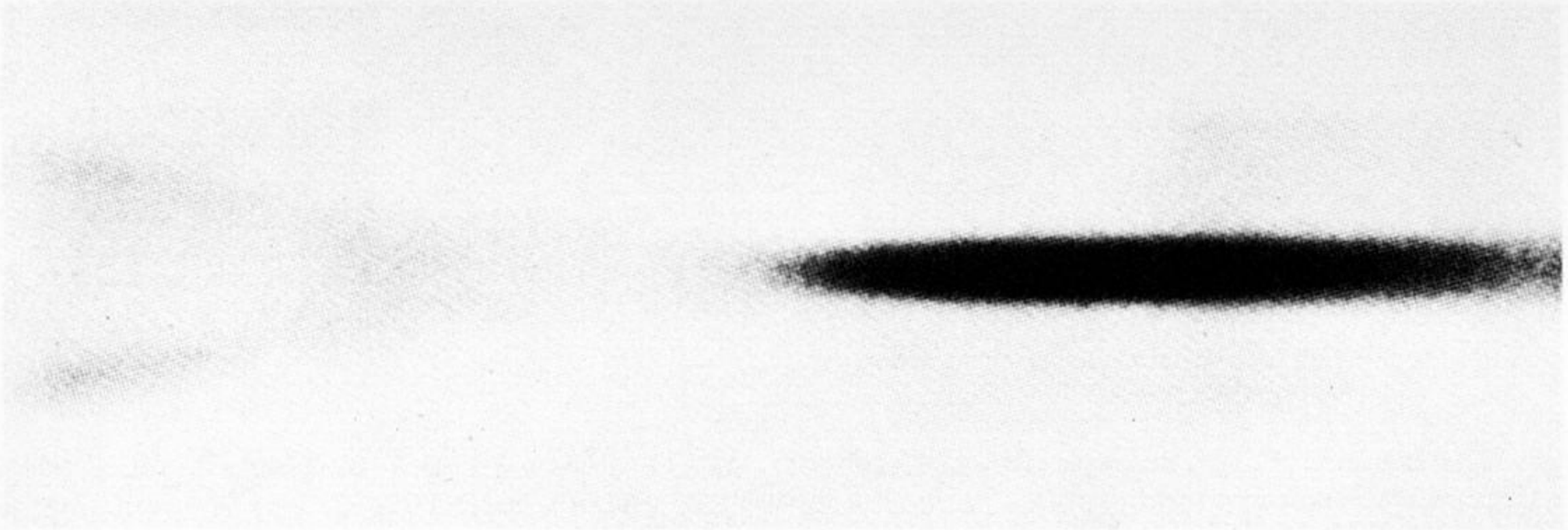

FIGURE 6. End-on streak picture in the Imperial College Mark II *Z*-pinch; pressure 70 mTorr H_2, current 60 kA, in Pyrex tube 8 cm long, 4 cm diameter.

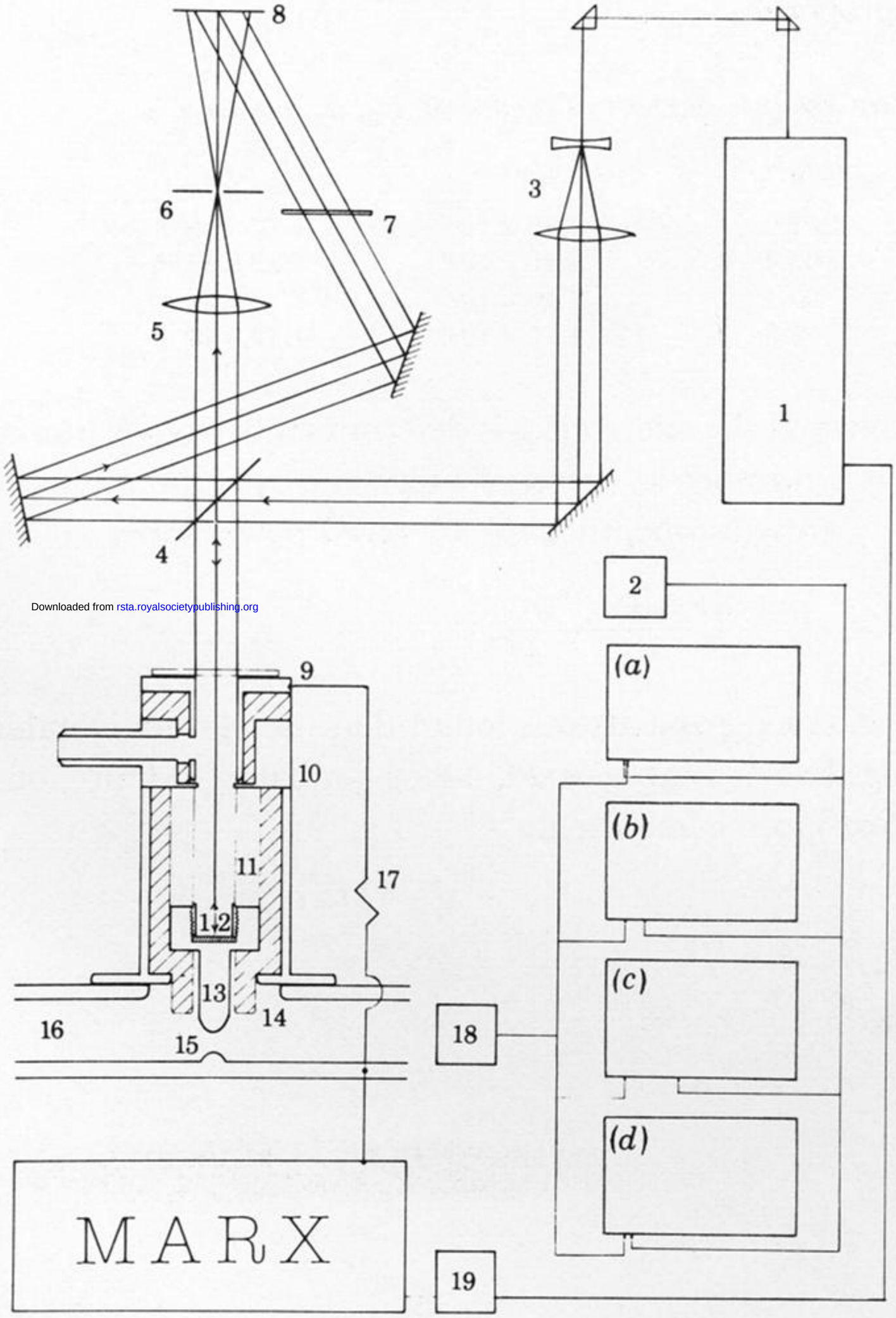

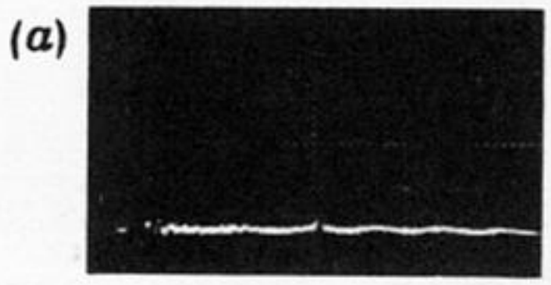

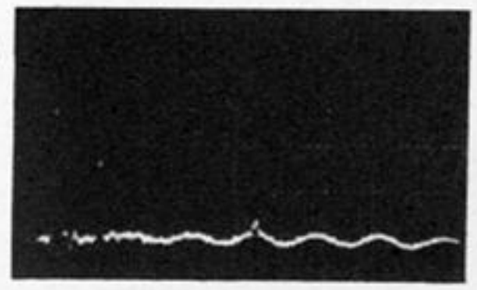

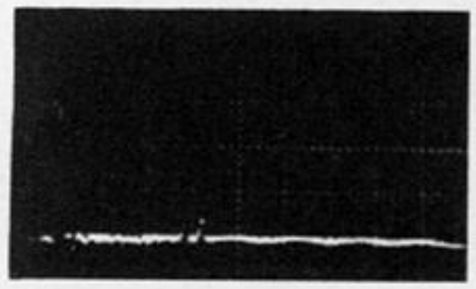

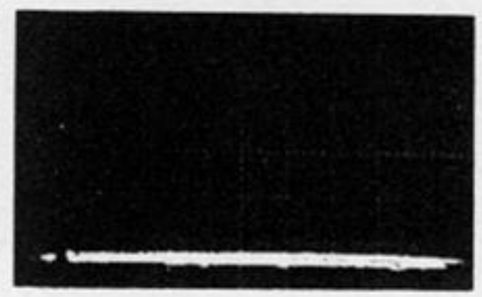

FIGURE 7. Arrangement for holographic interferometry. 1, Q-switched 30 mJ ruby laser; 2, pin diode laser monitor; 3, beam-expanding optics; 4, beam splitter; 5, imaging lens; 6, aperture; 7, beam alternator; 8, IOE75 film; 9, pre-ionization electrode; 10, Earth electrode; 11, pinch tube; 12, front surfaced mirror; 13, main electrode; 14, PTFE insulator; 15, water gap; 16, transmission line PFL; 17, $CuSO_4$ resistor; 18, water-gap optical monitor; 19, optical trigger to laser Pockel cell. Oscillographs (*a*)–(*d*) correspond with holograms (*a*)–(*d*) in figure 9.

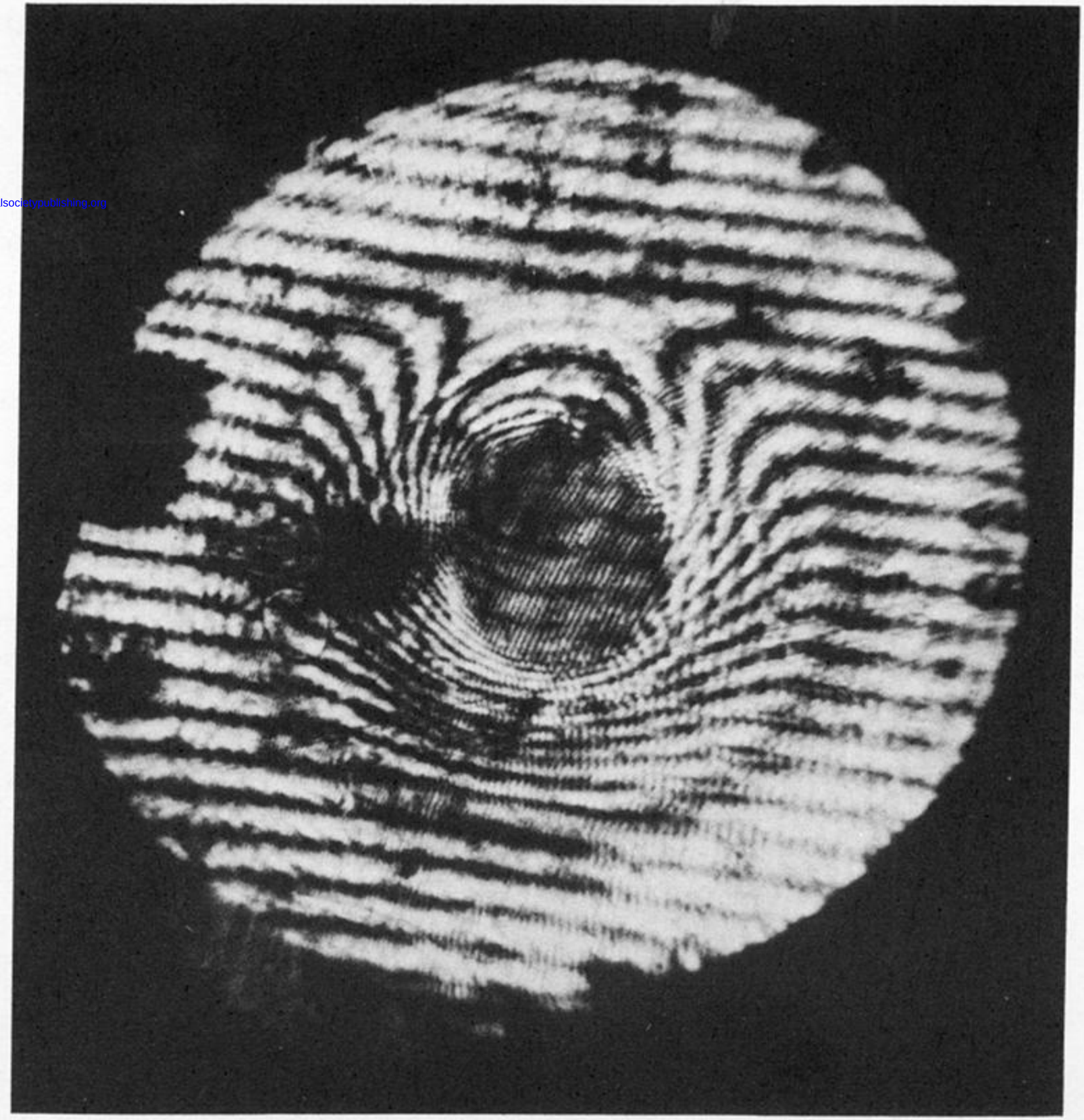

FIGURE 8. Holographic interferographic picture 350 ns after start of the current; tube radius 1 cm, length 5 cm, fill pressure 350 mTorr H_2, current 80 kA.

PHILOSOPHICAL TRANSACTIONS OF THE ROYAL SOCIETY A MATHEMATICAL, PHYSICAL & ENGINEERING SCIENCES

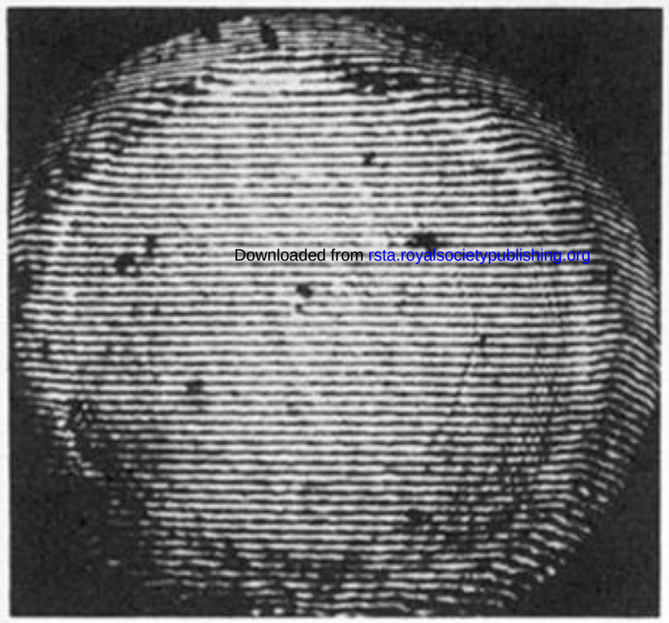

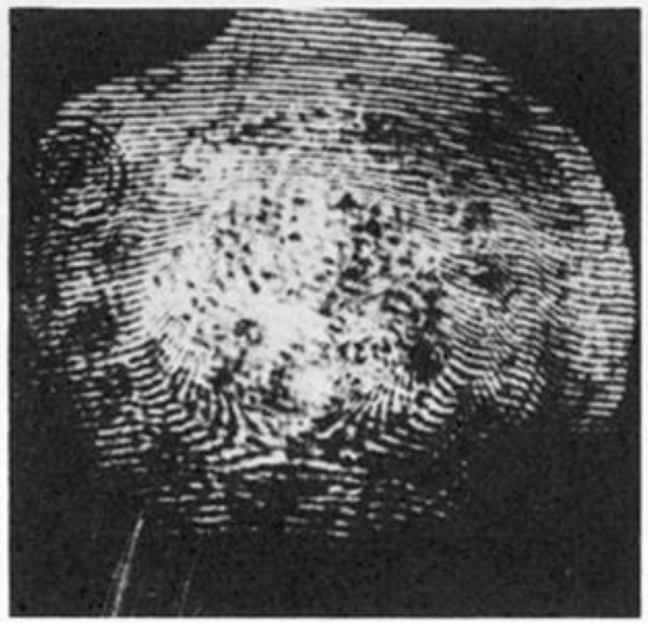

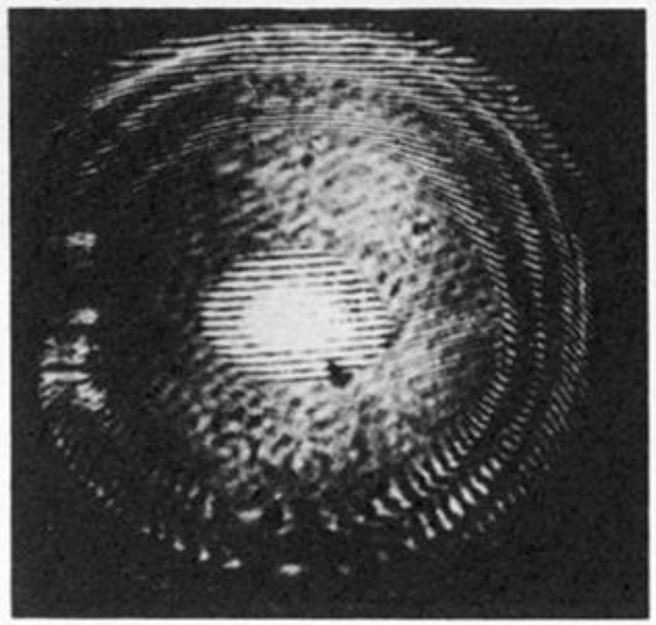

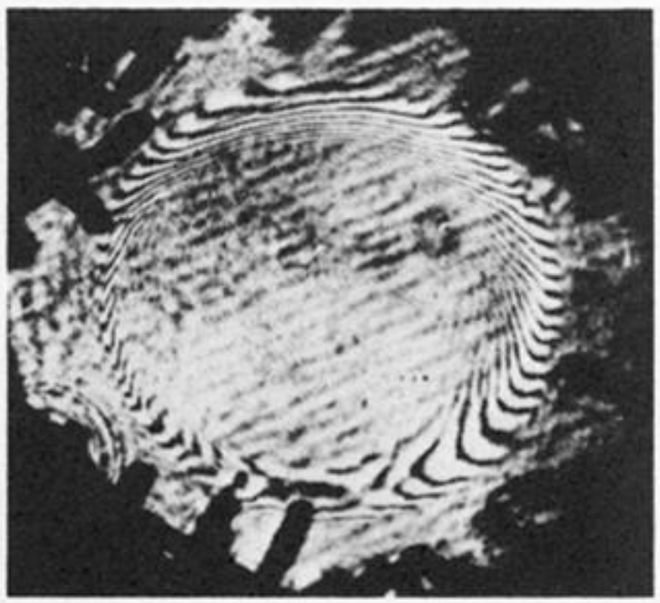

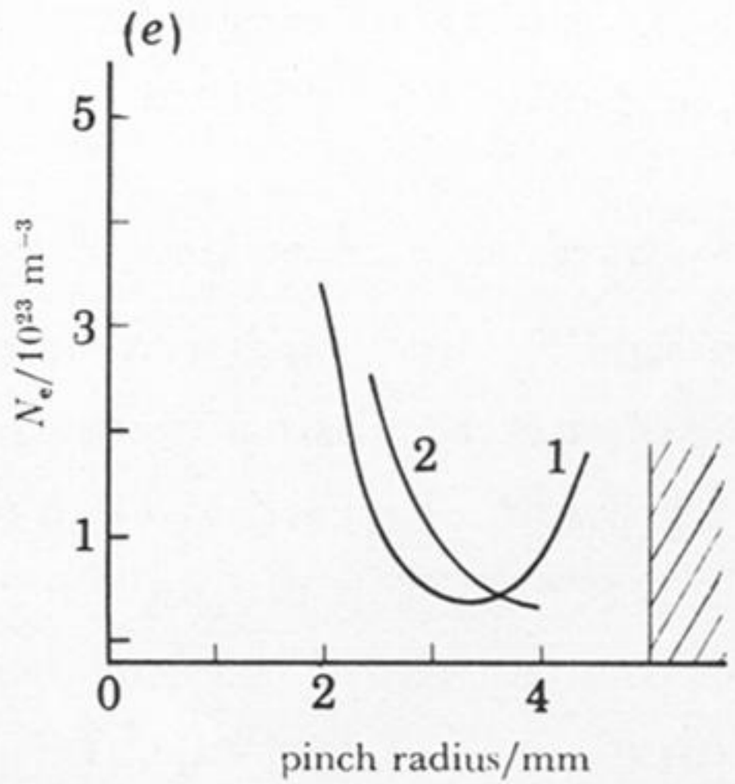

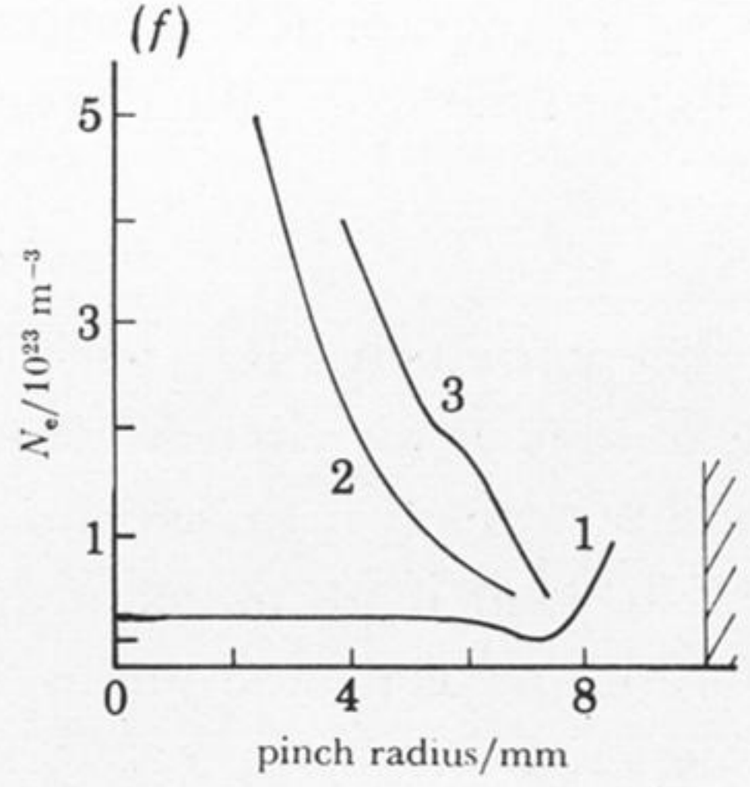

FIGURE 9. Series of holograms and density profiles (see text). The electron density profiles were calculated from the holograms by neglecting the contribution of neutrals to the refractive index.

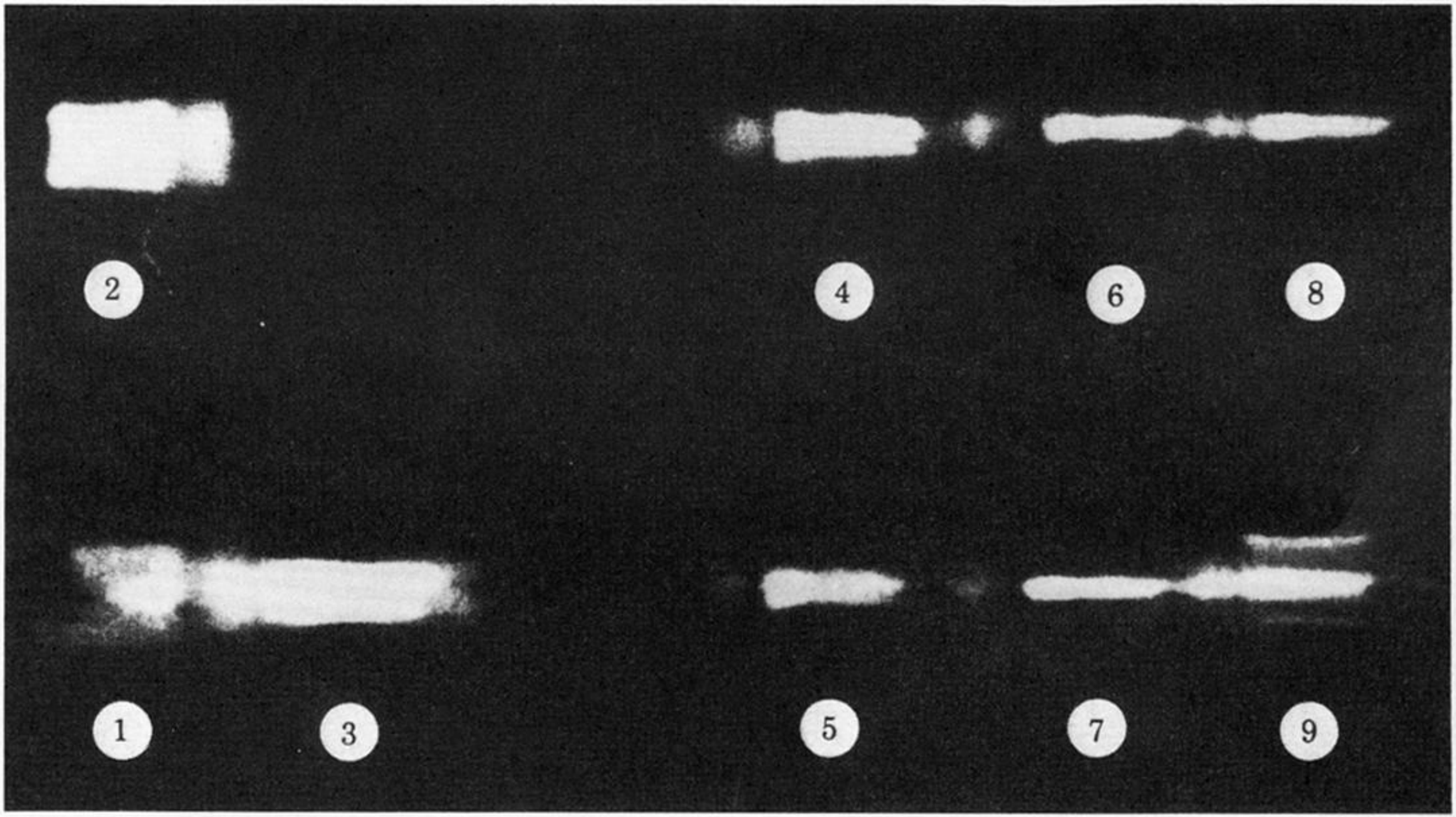

GURE 10. A sequence of side-on framing camera photographs taken on the Mark 1 *Z*-pinch. The exposure time is 10 ns, with 50 ns between successive exposures numbered in sequence. In each frame the light at each end of the main discharge is due to the pre-ionizers.

PHILOSOPHICAL TRANSACTIONS OF THE ROYAL SOCIETY A MATHEMATICAL, PHYSICAL & ENGINEERING SCIENCES

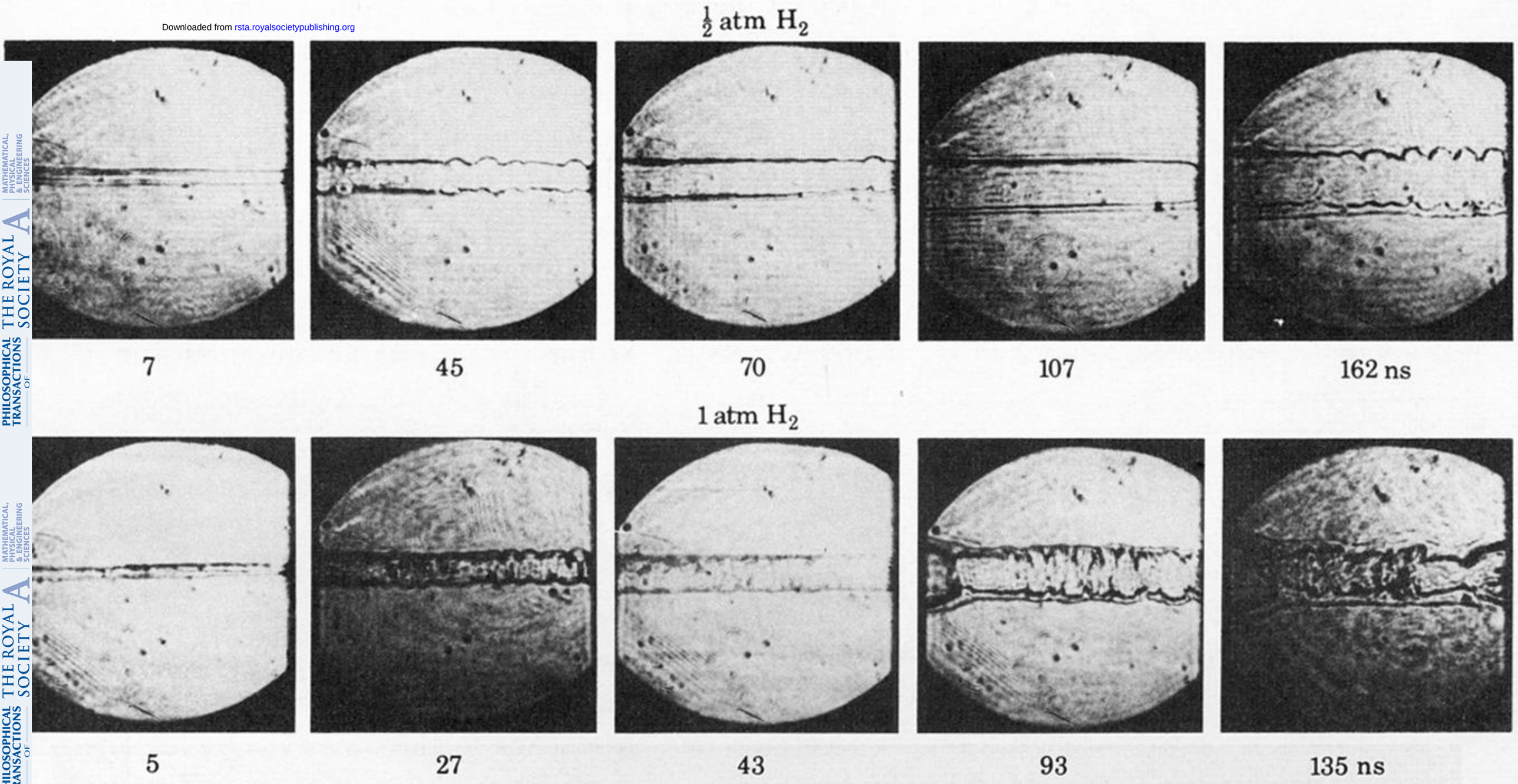

FIGURE 11. Sequence of side-on Schlieren interferograms, upper five at ½ atm H_2 and lower five at 1 atm H_2 (see text).

PHILOSOPHICAL TRANSACTIONS OF THE ROYAL SOCIETY A MATHEMATICAL, PHYSICAL & ENGINEERING SCIENCES

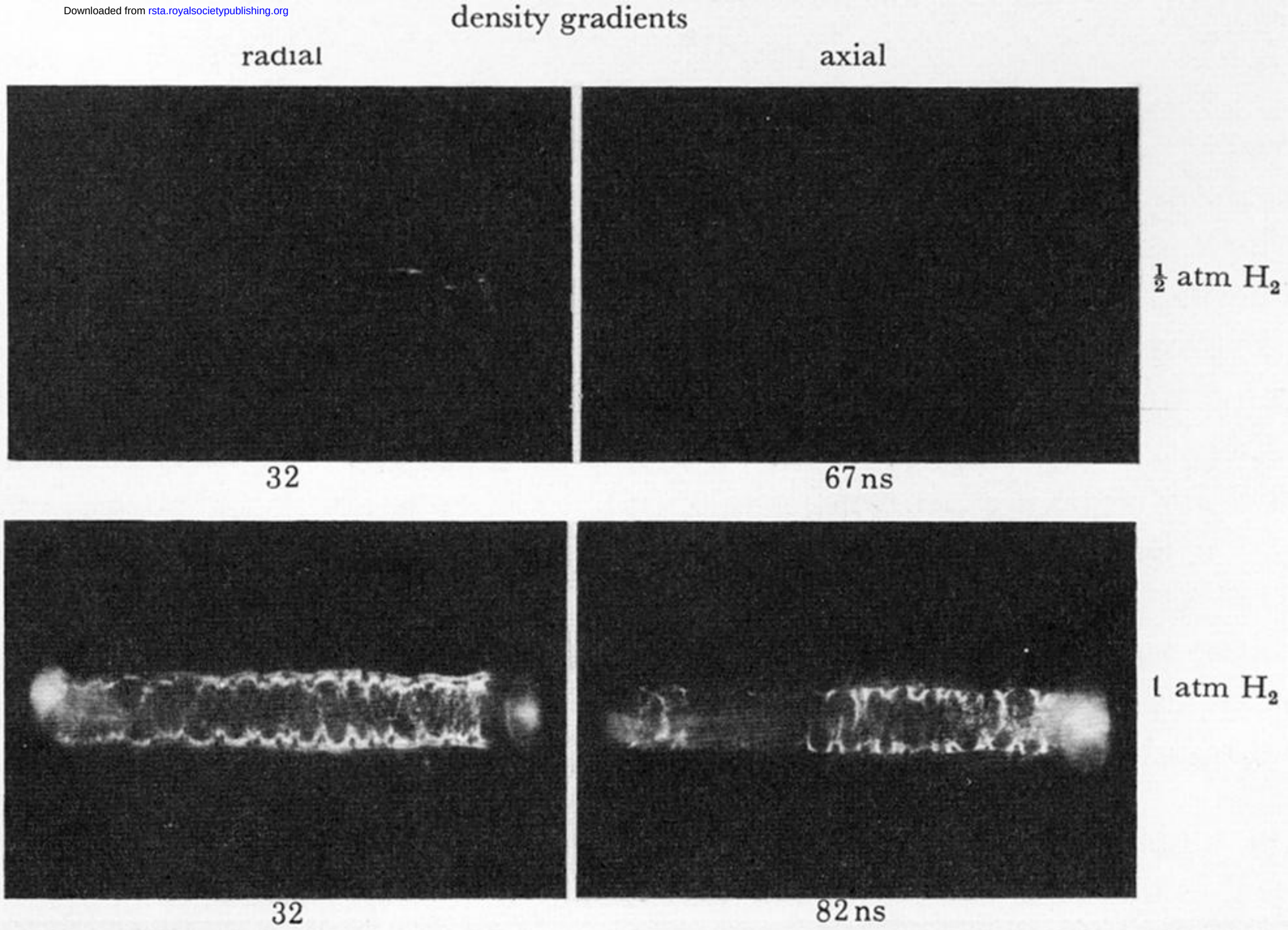

GURE 12. Dark-field schlieren interferograms of laser-initiated gas-embedded *Z*-pinch (see text).